QUANTIFYING THE EFFECT OF POSITION ERRORS IN SPHERICAL NEAR-FIELD MEASUREMENTS

Allen C. Newell, Greg Hindman

Nearfield Systems Incorporated
1330 E. 223rd St. Bldg. 524
Carson, CA 90745 USA

Abstract

Concise mathematical relations have been derived for Planar Near-Field measurements that quantify the effects of x, y and z-position errors on antenna parameters such as gain, sidelobe level, pointing, and cross polarization. Because of the complexity of the theory, similar relations for spherical near-field measurements have not been developed. The requirements for the spherical coordinate system are generally defined in terms of the alignment parameters such as orthogonality and intersection of axes, θ-zero, x-zero and y-zero rather than individual errors in θ, φ and r. Mechanical, optical and electrical techniques have been developed to achieve these alignments. This paper will report on the development of methods to estimate the antenna parameter errors that will result from spherical alignment errors for typical antennas.

Keywords: Antenna Measurements, Near-field, Spherical, Error Analysis, Simulation

1. Introduction

Mathematical analysis has been used with planar near-field measurements to derive the relationships between x-, y-, and z-position errors and the antenna parameters obtained from the near-field data. Given a minimum amount of information about the antenna, such as the measurement frequency, the antenna dimensions, and the aperture efficiency, we can easily estimate the uncertainty in gain, side-lobe level, cross-polarization, and beam pointing due to planar position errors[1]. Progress has been made[2], but the complexity of the spherical near-field transformations has thus far prevented similar success for spherical measurements. In the absence of analytical error equations, we must use more time consuming methods[3] to obtain estimates of uncertainty. One approach has been to induce specific alignment errors and observe the change in resulting far-field parameters for specific antennas. In a previous paper[4], we identified the alignment errors that are common to all spherical measurement systems and

developed electrical tests to aid in adjusting the mechanical rotator system. This paper reports on experimental work to develop general guidelines for how accurate each alignment parameter must be. The approach was to induce know alignment errors in a precisely aligned spherical measurement system and obtain spherical near-field data for incremental changes in each alignment parameter. Comparing the results from known misalignment data with the results from unperturbed data provided a measure of the error level in the far-field parameters. This was done for a broad-beam horn and a narrow-beam slotted array so the effect of antenna type could be assessed. The results provide a first step at providing guidelines for spherical measurement system alignment.

2. Measurement System

A correctly aligned spherical measurement system is shown in Figure 1.
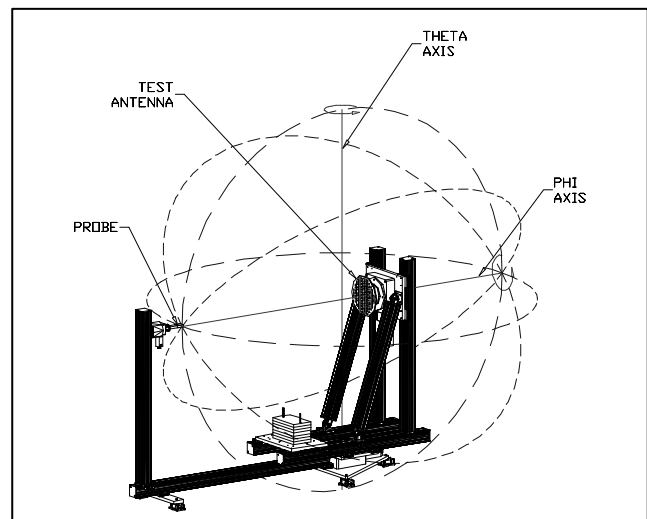
Figure 1 Correctly aligned spherical measurement system.

The measurement system was first aligned using the

electrical tests on a 15 dB gain X-Band horn. The horn and probe are shown in Figure 2 with the horn offset for the Y-
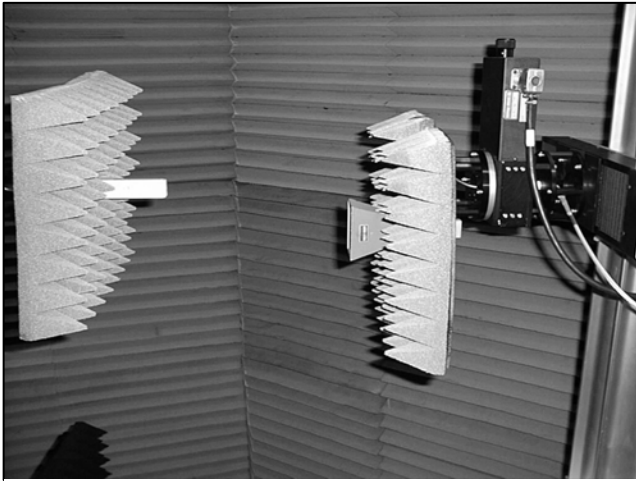
Figure 2 X-Band horn on spherical measurement system.

Zero alignment test. When the alignment was completed, the horn was placed with its axis approximately coincident with the φ-axis of the rotator and its main component approximately along the X-axis.

The alignment errors that were induced during these tests are:
1- Non-orthogonality of the θ and φ axes;
2- Y-zero error;
3- θ-zero error;
4- X-zero error;
5- Non intersection of the θ and φ axes;
6- Probe axis not parallel to the z-axis.

Measurements with errors 2, 4 and 5 were obtained in an automated sequence of 21 separate spherical scans. The sequence began with two data sets with no errors induced that served as the baseline reference. Four data sets were then acquired with X-Zero errors of 0.01, 0.02, 0.05 and 0.10 inches. This was followed by a set with no errors to measure repeatability. Four sets were then obtained with Y-Zero errors of 0.10, 0.20, 0.50, and 1.00 inches respectively and then a return to the no-error state. Four non-intersection error sets were then obtained with errors of 0.01, 0.02, 0.05, and 0.10 inches, followed by a return to the no-error state. For each non-intersection error, the probe was moved in x by the same amount so the probe remained along the φ-axis. The final 4 measurement sets were with Δx=0.02 , Δy=0.20, non-intersection=0.02 in., and no errors respectively. All of these were automated using the NSI software and spherical measurement system. The θ- and φ-rotators were run at slow speed to reduce extraneous position errors, and the total measurement took

about 10 hours for the 21 data sets.

The remaining errors were induced manually using shims or manual reset of positioners. Measurements on the horn were performed at 8.5, 9.34 and 12.0 GHz. Measurements on the X-Band slotted array, with a gain of about 30 dB, were performed at its center operating frequency of 9.34 GHz.

3.0 Data Analysis, Automated Data Sets

We first compared the zero-error data sets taken before and after each error sequence to determine system drift and repeatability. This established a baseline level for the error signal that will be determined in the following analysis. We then used the zero-error data set that was taken immediately prior to a block of induced errors as the reference for that block. For instance, data set 7 with no errors was compared to data sets 8-11, which had Y-zero errors, and data set 12 was compared to data sets 13-16 which had non-intersection error. In each of these comparisons, the far-field patterns were obtained and the principal plane patterns were plotted for both main and cross components. An error signal pattern was then computed by taking the difference in the amplitudes and determining the error signal that would cause the observed difference. Sample results are shown in Figures 3-6. In addition to the principal plane cuts produced for all measurements, a limited number of cuts at φ = 45 degrees and contour plots over the full hemisphere were also
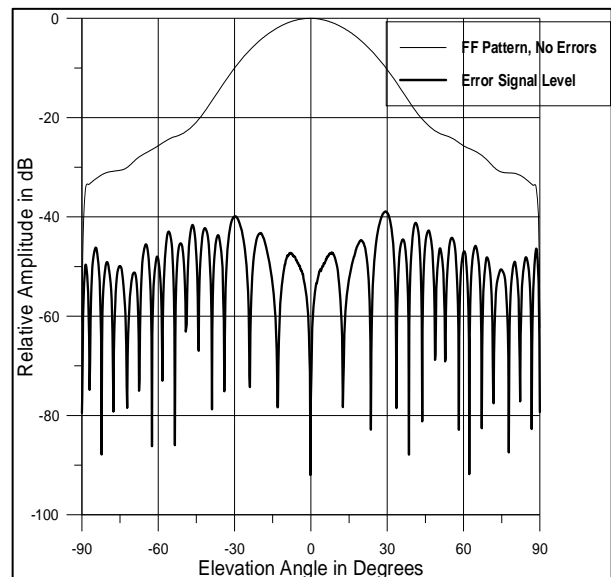
Figure 3 Results of processing spherical near-field data on X-Band horn showing H-Plane, principal polarization, far-field pattern and error signal level due to non-intersection error of 0.05 inches.

produced to verify that the principal planes were representative of the full region. From these and similar results for the different errors we obtained an estimate of the change in on-axis gain and directivity and the error signal level for the principal polarization over the main-beam, in the sidelobe region and for the cross-polarized component in the main-beam and side lobe regions.
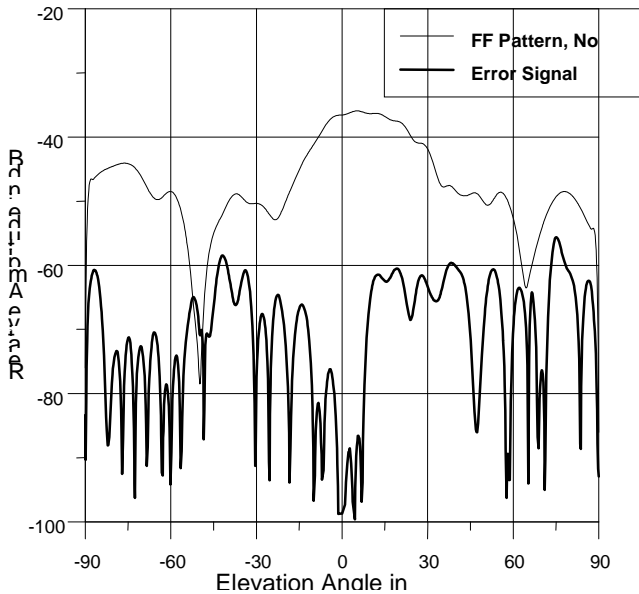
Figure 4 Results of processing spherical near-field data on X-Band horn showing H-Plane, cross polarization, far-field pattern and error signal level due to non-intersection error of 0.05 inches.
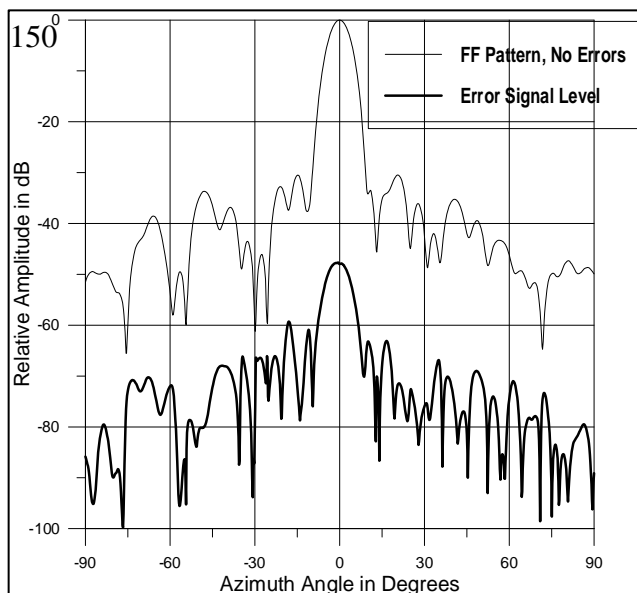
Figure 5 Pattern and error level results for X-Band slotted array, principal component. Non-intersection error = 0.05 inches.
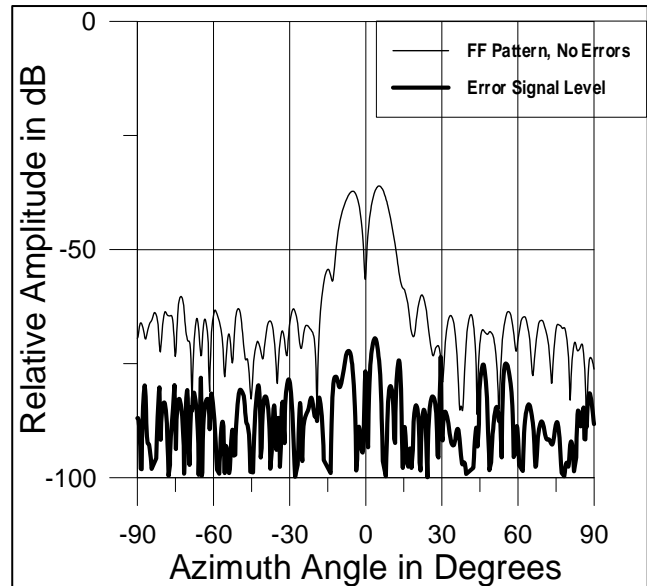
Figure 6 Cross-component pattern and error level results for X-Band slotted array. Non-intersection error = 0.05 inches.

Figure 7 is a sample of the final results from the error simulation. This shows that the results for the horn at two different frequencies and the array are very similar. This curve could be used for spherical measurements on antennas up to 30 dB with high confidence. Since there is so little difference between the horn and the array results, it can probably be applied to antennas with higher gain.
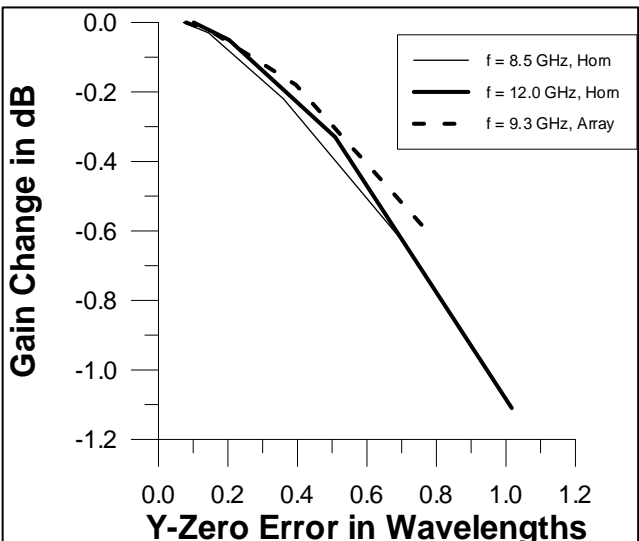
Figure 7 Graphical summary of error simulation results showing gain change versus Y-zero error.

It was initially assumed that the Y-zero error would have a smaller effect than the others would since its effect is more difficult to see in the electrical alignment tests. However, Figures 7, 8 and other results for the Y-zero error indicates
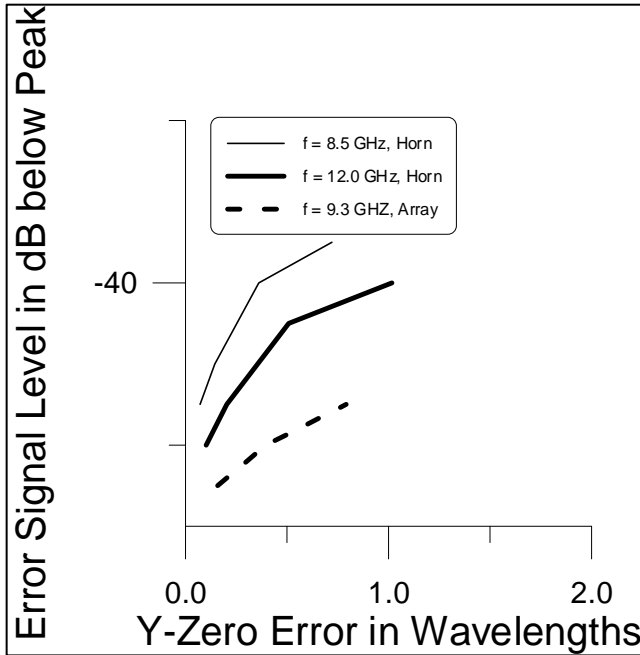
Figure 8 Graphical summary of error simulation results showing error signal level in cross-polarization versus Y-zero error.

that ΔY-zero must be less than 0.2 λ for reliable results. In contrast to Figure 7, Figure 8 shows that the cross-polarized error does depend on the antenna. This could use further study. Graphs similar to Figure 8 were produced for main beam and side lobe errors and these will be presented at the conference.

It was anticipated that X-zero and non-intersection errors would have a larger effect on the results than the Y-errors, and therefore they were varied over a maximum of 0.1 inches rather than 1.0 in. Figure 9 for non-intersection errors shows that this error must be smaller than y-errors, but it would also be useful to have data over a larger range of values. The effects for errors of 0.01 and 0.02 inches were usually below the repeatability level of the no-error data sets.

One result from the non-intersection study is especially interesting since there are other results to compare with. Dich and Gram [5] of the Technical University of Denmark reported on a combined mathematical simulation and measurement study that showed extreme sensitivity to non-intersection errors. They focused on the effect this error
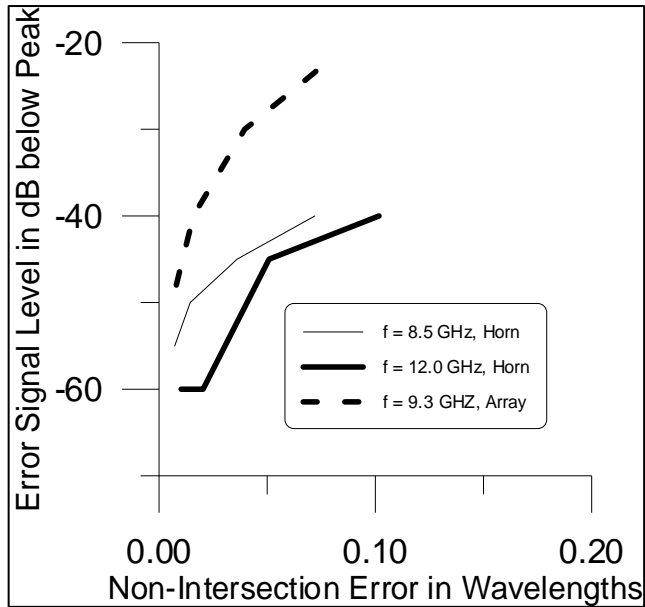
Figure 9 Graphical summary of error simulation results showing error signal level in main beam region due to non-intersection error.

has on directivity. Their results along with the results of the present study are shown in Figure 10. It is not apparent why the two results are so different, but it does illustrate the complex nature of the spherical near-field measurements. It
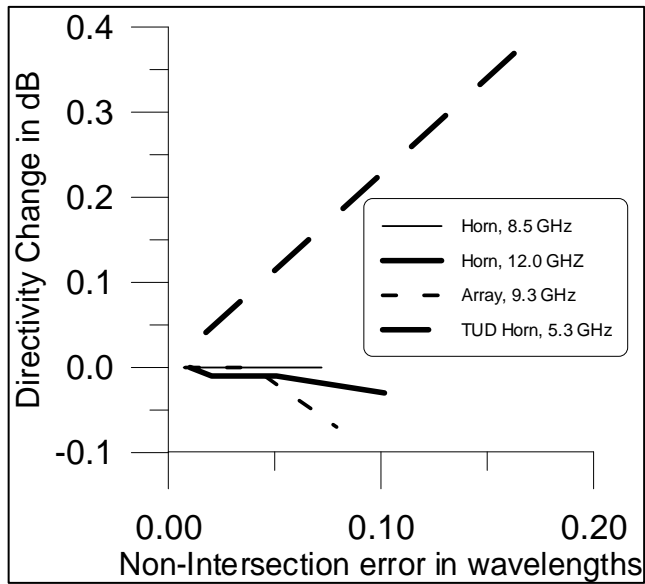
Figure 10 Effect of non-intersection error on directivity results.

also shows that caution must be used in extending results of an error study on a specific antenna and measurement situation too broadly. Possible reasons for the difference are: 1- The TUD measurements were made on very large

radii of 6 and 12 meters compared to the 0.3 m radius used here. 2- The probe in the TUD measurement may not have been moved in x when the ϕ-axis was translated to produce the non intersection error. This would give a combination of two errors. 3- Some parts of the numerical analysis may be different. This also should be studied further to resolve the reason for the differences. 4- The small range of errors in our study may not be large enough to show the correct trend. This seems unlikely however since all the results show the same characteristic of either no change or a decrease in directivity with error.

4. Conclusions

Results similar to the above figures have been obtained for all of the alignment error sources. These will be presented in the conference presentation. They will serve as a basis for alignment requirements and error estimates for a broad range of measurements, and with additional studies could be made quite general.

5.0 References

[1] A. C. Newell, "Error Analysis Techniques for Planar Near-Field Measurements", *IEEE Trans. Antenas Propagat.*, AP36, No. 6, June 1988, pp. 754-768.

[2] L. A. Muth, "Displacement Errors in Antenna Near-Field Measurements and their effect on the far-field", *IEEE Trans. Antenas Propagat., AP36, No 5, May 1988, pp 581-591*.

[3] D. J. Janse van Rensburg, R. S. Mishra, G. Seguin, "Simulation of Errors in Near-field facilities, *In the proceedings of the 17th annual AMTA Meeting and Symposium*, pp336-340, Williamsburg VA, USA, 1995

[4] A. C. Newell, G. Hindman, "The alignment of a spherical near-field rotator using electrical measurements" *In the proceedings of the 19th annual AMTA Meeting and Symposium,Montreal, Canada, 1997.*

[5] M. Dich, H. E. Gram, "Alignment errors and standard gain horn calibrations", In the proceedings of the 19th annual AMTA Meeting and Symposium , pp 425-430, Montreal, Canada, 1997.